Elastic layer thickening with age of the oceanic lithosphere: a tool for prediction of the age of volcanoes or oceanic crust

S. Calmant,[1] J. Francheteau[2] and A. Cazenave[1]
[1] *CRGS/CNES, 18 av. E. Belin, 31055 Toulouse cedex, France*
[2] *Institut de Physique du Globe, 4 pl. Jussieu, 75252 Paris cedex 05, France*

SUMMARY

To first order, the estimated thickness T_e of the elastic part of the oceanic lithosphere increases linearly with the square root of the age of the lithosphere at the time of loading, Δt. In order to quantify this relationship in the particular case of volcanic loading, a synthesis of T_e estimates reported both in this paper and in previous studies is conducted. Excluding the anomalously low estimates from the south-central Pacific, the values are very consistent for the three main oceans and follow the empirical relationship: T_e (km) = $(2.7 \pm 0.15)\sqrt{\Delta t}$ (Ma). The relationship is used to predict the age of volcanoes when the age of the crust is known (for the Trindade chain in the south Atlantic Ocean) and to predict the age of the crust when the age of the volcanoes is known (for the Pacific plate east of the Tonga trench). The age estimates are in good agreement with the structural setting.

Key words: age prediction, elastic thickness, oceanic lithosphere, volcanoes.

INTRODUCTION

Elastic flexure theory has been successfully applied to model the response of the oceanic lithosphere to loading of volcanic chains and seamounts (e.g. Walcott 1970; Watts & Cochran 1974; Watts, Cochran & Selzer 1975; Watts 1978, 1979; Cazenzve *et al.* 1980; Watts & Ribe 1984). A linear relationship between the square root of plate age at the time of loading and the thickness of the elastic lithosphere was found by Watts (1978) [see also Watts, Bodine & Ribe (1980)]. Knowledge of the relationship may have important potential applications. It was used by Watts *et al.* (1980) to infer the tectonic setting of a number of volcanoes at the time of their formation: a small elastic thickness indicates that they formed on or near ridges while a large elastic thickness corresponds to off-ridge formation. The relationship can also be used to infer either the age of the plate, when the age of volcanoes loading the plate is known, or the age of volcanoes, when the age of the plate which is loaded is known. However, the relationship is not sufficiently constrained because of the small number of elastic-thickness estimates and the mixing of estimates from volcano loading with those for subducting plate deformation.

We have undertaken a global study in order to determine the elastic thickness under oceanic volcanoes at the maximum number of sites. We used a 3-D model of flexure constrained by geoid height data from the SEASAT satellite which offers global coverage, hence systematic determinations, provided that the age of both plate and volcanoes are known. A total of 38 elastic-thickness estimates have been obtained for the Pacific Ocean. The results are published in Calmant & Cazenave (1986) and Calmant (1987). 17 new estimates are proposed for the Atlantic and Indian Oceans. The purpose of this paper is to report the latter results and to propose a new relationship between elastic thickness and age of plate at time of loading, valid on a global scale, except over the south-central Pacific Ocean where a broad anomaly (anomalously small thicknesses) has been identified (Calmant & Cazenave 1987). The relationship is used as a tool to predict either plate or volcano ages. The prediction is applied in two selected areas.

T_e ESTIMATES

The elastic part of the lithosphere has been modelled using the thin elastic plate theory. In order to apply the theory to the oceanic lithosphere, it is assumed that the upper boundary of the elastic layer is close enough to the surface that the deformation of the elastic layer mimics the shape of the Moho. The other main assumptions are that the deformations are small and that the stresses induced by the overburden can be neglected.

The symbols used in the following equations refer to parameters defined in Table 1.

Subject to a vertical force Q per unit area, the plate will react by a deflection w given by

$$D \nabla^4 w = Q \tag{1}$$

where D is the flexural rigidity, related to the thickness T_e of

Table 1. Numerical values of geophysical parameters.

Density:	Sea water	ρ_w	= 1.03
	Load	ρ_v	= 2.8
	Infill	ρ_s	= 2.8
	Crust	ρ_c	= 2.8
	Mantle	ρ_M	= 3.4
Mean gravity		g	= 9.81 m/s^2
Crustal thickness		t_c	= 6 km
Young's modulus		E	= 10^{12} N/m^2
Poisson's ratio		v	= 0.5

the layer through

$$D = T_e^3 \frac{E}{12(1 - v^2)} \qquad (2)$$

where e is Young's modulus and v is Poisson's ratio. Applied to the oceanic lithosphere, (1) must be rewritten according to the three components of Q: (*i*) the infill of the flexural moat by sediments (density ρ_s), (ii) the restoring force due to replacement of mantle material (density ρ_M) by lighter crust (density ρ_c) as the Moho is deflected downward and (iii) the load P of the volcano itself (density ρ_v). Replacing the contributions (i) and (ii) by their expressions $gw(\rho_s - \rho_c)$ and $gw(\rho_c - \rho_M)$ respectively, (1) becomes:

$$D\nabla^4 w + gw(\rho_M - \rho_s) = P \qquad (3)$$

The expression for the load P will be different for undersea volcanoes and islands. P is determined by the height of the volcanic structure, as given by the bathymetry $H(x, y)$. Assuming a basement depth B (depth of the seafloor from the load), P will be (water density is ρ_w and H is positive downward) given by

$$P(x, y) = g(\rho_v - \rho_w)[B - H(x, y)] \text{ for a submarine volcano,} \qquad (4)$$

$$P(x, y) = g(\rho_v - \rho_w)B - g\rho_v H(x, y) \text{ for an island.} \qquad (4')$$

In the SYNBAPS data base (Van Wickhouse 1973), bathymetry is given on 5 min × 5 min regular grid. The numerical integration of the plate deflection is computed on this grid. The solutions of (3) given by Watts et al. (1975) have been used. For each volcano, the total area of computation is 7–25 square degrees, centred on the volcano. The area has been kept as small as possible while still including the flexural moats and the whole geoid signature of the volcano. The deflection has been computed on the same grid as the bathymetry for a large variety of D values, ranging from 5×10^{20} to 10^{24} N m. The effects on the geoid height N of the geometry of the load and the associated deflection result in two opposite contributions; a positive fixed contribution (depending only on the density of the load ρ_v) and a negative D-dependent contribution of the crust–mantle interface. Each contribution δN has been calculated using the following equation, derived from Brun's formula;

$$\delta N(P, P') = \frac{G}{g} \int_\omega \frac{\Delta\rho}{r} d\omega \qquad (5)$$

where r is the distance between the mass anomaly (of

volume ω centred on P and characterized by a relative density contrast $\Delta\rho$) and the point P′ of the surface where the geoid height is calculated. Setting $\omega = \Delta R \, \Delta S$ where ΔS is the grid step surface and ΔR the height of the column of constant density contrast $\Delta\rho$, (5) becomes

$$\delta N(P, P') = \frac{G}{g} \Delta S \, \Delta\rho \int_R^{R+\Delta R} \frac{R^2 \, dR}{(a^2 + R^2 - 2aR \cos \Theta)^{1/2}} \qquad (5')$$

in spherical coordinates, where a is the Earth's radius (since P′ is at the sea surface), R is the distance from P to Ω—the centre of the Earth—and Θ is the angle between ΩP and ΩP′. The integrated form of (5′) is

$$\delta N(P, P')$$
$$= \frac{G}{g} \frac{\Delta\rho \, \Delta S}{2} \left[(R + 3a \cos \Theta)(R^2 + a^2 - 2aR \cos \Theta)^{1/2} \right.$$
$$\left. - a^2(1 - 3 \cos^2 \Theta) \operatorname{arcsinh} \left(\frac{R - a \cos \Theta}{a |\sin \Theta|} \right) \right]. \qquad (5'')$$

To constrain D, the computed geoid heights have been compared with the altimetric data provided by the SEASAT satellite. The data are along-track values, averaged on a footprint 2 km across by 7 km along the track. At short wavelengths, data precision is to about 10 cm. The data are thus well adapted to study the seamount geoid signatures which are several hundreds of km in length and up to 10 m in amplitude. The spacing in geoid height samples is close to the grid step which ranges from 5 to 9 km, according to the latitude. The computed geoid heights are provided, for each D value, on the same grid as the bathymetry and the deflection. They have been projected along the satellite tracks using a Lagrangian interpolator. This was conducted for each track crossing the local map close enough to the summit of each volcano. A study on a restricted surface results in a high-pass filter in geoid heights. The long wavelengths ($\geqslant 1000$ km) in the altimetric data have thus been removed using the GRIM3-L1 global potential model (Reigber et al. 1985) developed in spherical harmonics up to degree and order 36.

VOLCANOES

From the good fit between predicted and observed geoid heights (Fig. 1), T_e has been successfully determined for 46 volcanoes along linear chains and for 13 individual volcanoes (see Table 2). The unequal distribution of the listed volcanoes (Fig. 2) reflects the difference in volcano distributions within the three oceans. The Pacific Ocean bears long chains of well-separated volcanoes, the Indian Ocean mainly plateaus or continuous ridges, while both are equally present in the Atlantic Ocean. As our model is not adapted for the study of large elongated structures, the Pacific features were the most appropriate for this kind of analysis. In the Pacific Ocean, the Hawaii–Emperor, Marquesas, Pitcairn, Society, Cook–Austral, Samoa and Easter chains have been studied by Calmant & Cazenave (1986) and Calmant (1987). Here, new results are reported for the Azores, Bermuda, Maderia, Ascencion and Santa Helena islands, Cruiser and Great Meteor seamounts and for the New England (Atlantic and Corner) and Cap Verde (Boa Vista and Santo Antao) chains in the Atlantic Ocean,
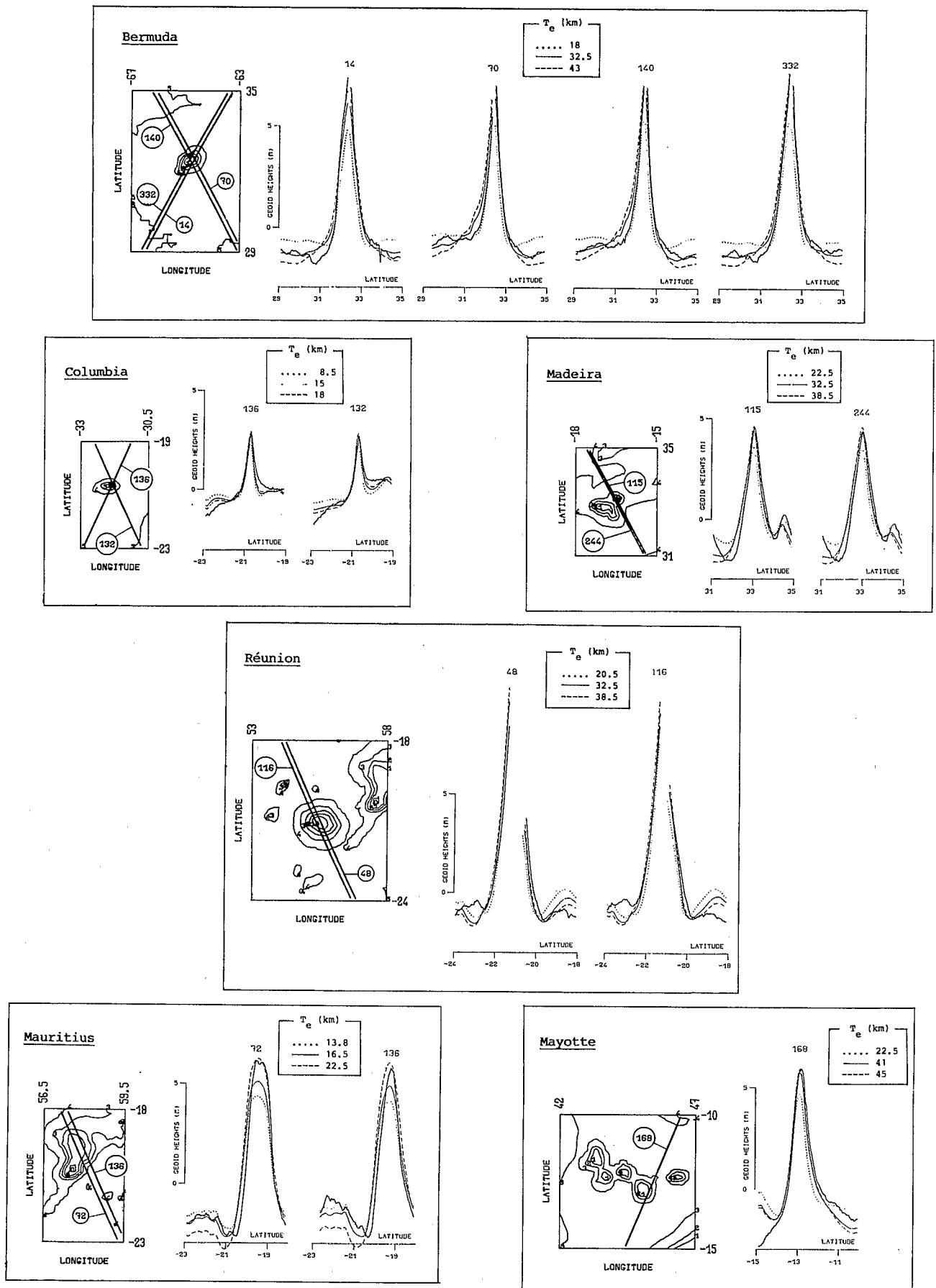
Figure 1. Comparison between observed and computed geoid heights for a set of six volcanoes; Bermuda, Columbia and Madeira in the Atlantic Ocean, Réunion, Mauritius and Mayotte in the Indian Ocean. Left; bathymetric map used for computations and location of the SEASAT tracks. Right: observed (SEASAT data) and computed (along-track extrapolated) geoid heights.

Table 2. Volcanoes presented in this study with the value of elastic thickness (T_e), age of plate (t_p) and age of volcano (t_v) used—south-central Pacific excepted—to determine (6).

Location		Age of plate (Ma)	Age of volcano (Ma)	Elastic thickness T_e (km)
Atlantic Ocean				
Atlantis	38 °N 63.9°W	170	95	22.5±2
Azores	37.8°N 25.5°W	32	30	< 6
Corner	36.5°N 51.5°W	98	73	6 ±1
Madeira	33 °N 17 °W	129	1	32.5±4
Bermuda	32.4°N 64.8°W	117	30	32.5±8
Cruiser	32 °N 28.2°W	70	60	7 ±1
Great Meteor	30 °N 28.5°W	80	14	19 ±2
Cape Verde	17.1°N 25.2°W	116	10	21 ±2
Cape Verde	16.1°N 22.7°W	140	10	30 ±5
Ascencion	7.9°N 14.4°W	7	2	7 ±1
St Helena	16 °S 5.7°W	41	16	9.5±3
Indian Ocean				
Mayotte	12.9°S 45.2°E	150	5	40.5±4
Rodriguez	19.6°S 63.5°E	10.6	1.5	< 6
Mauritius	20 °S 57.7°E	59	8	16.5±1.5
Réunion	21.2°S 55.5°E	64	2	32 ±5
Crozet +	46 °S 51 °E	80	5	22.5±2
P. Edward	47 °S 38 °E	39	0	16.5±3
Pacific Ocean +++				
Hawaiian chain				
Kauai	22 °N 159.5°W	93.5	5	32.5±1.5
Niihau	22.8°N 161 °W	94.5	6.5	28 ±2.5
Nihoa	23 °N 162 °W	97	7.5	21.5±1.5
Necker	23.5°N 164.5°W	100	10.5	26 ±2.5
Raita Bank	25.5°N 159.5°W	108	17	21.5±1.5
Gardner pin.	25.5°N 168 °W	106	15	25.5±1.5
	25.5°N 172 °W	110.5	19.5	22.5±1.5
	25.5°N 170.7°W	112	18	28 ±1
	26.5°N 174.5°W	114.5	22.5	26.5±2
Lisianski	26 °N 174 °W	114	22	25.5±3
Pearl Hermes	28 °N 176 °W	116.5	20.5	27 ±2.5
Midway	29 °N 179 °W	119	27	26.5±2.5
	31 °N 176 °S	127	35	20 ±2
Kanmu	32 °N 173 °E	121	40	24.5±1.5
Emperor chain				
Diadakuji	32 °N 172.3EW	123	41.5	25.5± 6
Koko	35 °N 171.5°E	118	46.5	19 ± 1
Ojin	35.5°N 171.5°E	118	55	19 ± 2
Nintoku	41 °N 170.5°E	110	56	22.5±3.5
Suiko	45 °N 170°E	117	64.5	18 ±1.5
Jimmu	46.5°N 169.5°E	113	65	20 ± 2
Pitcairn chain				
Pitcairn	23.9°S 130.8°W	23	1	< 6
Gambier	23.2°S 135 °W	29.5	6	6 ± 1
Mururoa	22 °S 139 °W	35	7	6 ± 2
Easter chain				
Easter	27 °S 109 °W	4.5	0.3	< 6
Sala y Gomez	26.5°S 107.3°W	6	1.7	< 6
Cook Austral chain				
Mac Donald	29 °S 140.2°W	43	0	< 6
Rapa	27.5°S 144.5°W	52	5	< 6
Raivavae	24 °S 147.5°W	65	6.5	11 ± 2
Tubuai	13.3°S 149.5°W	70	9.5	8 ± .5
Rimatora	22.7°S 153.7°W	78.	13.5	12.5± 2
Maria	22 °S 154.7°W	80	15	10.5± .5
Atiu	20 °S 158.2°W	87	4	10 ±1.5
Mauke	20.1°S 157.3°W	85	5	12 ±1.5
Aitutaki	18.7°S 159.8°W	87	7	10.5±1.5
Rarotonga	21.2°S 159.8°W	87	1.5	15 ±1.5
Mangaia	21.9°S 157.9°W	85	17.7	7 ± .5
Society chain				
Tahiti	17.6°S 149.5°W	71	1	20 ± 2
Bora Bora	16.6°S 151.3°W	75	3	15 ±1.5
Maupiti	16.4°S 152.3°W	76.5	4	14 ± 1
Marquesas				
Central group	9.4°S 139.5°W	63	3	14 ± 2
Samoa				
Manuae	14.2°S 169.5°W	100	0	24 ±2.5
Louisville Ridge ++				
Valerie Guyot	41.5°S 164.3°W	85	35	18 ±1.5

+ Cazenave et al., 1980.
++ cazenave and Dominh, 1984
+++ Calmant, 1987; Calmant and Cazenave, 1986

as well as for the Réunion, Mauritius, Rodriguez, Prince Edward and Mayotte islands in the Indian Ocean.

For all the listed volcanoes of the Atlantic and Indian oceans (except Rodriguez) a hotspot origin has been proposed in the literature whether they belong to a well-developed chain (New England seamounts) or to a line of sparse volcanic features (Bermuda). The volcano ages can be found in McDougall & Chamalaun (1969), Duncan (1981, 1984), Morgan (1981), Emerick & Duncan (1982), Harris Bell & Atkins (1983) and Young & Hill (1986). In both oceans, plate ages are interpolated from *The Bedrock Geology of the World* (Larson et al. 1985), except for the Atlantis and Corner seamounts where more precise plate ages are reported in Duncan (1984) and for Rénunion Island where a more accurate value was provided by P. Patriat (personal communication). Table 2 displays the T_e estimates and the plate and volcano ages. In this table, estimates for Crozet (south Indian Ocean) and Valerie Guyot (Louisville ridge, south Pacific) are included since they were studied previously By Cazenave et al. (1980) and Cazenave & Dominh (1984) using a similar method.

Unsuccessful studies have been conducted for Ob, Lena and Marion Dufresne seamounts, Comores (except Mayotte) and Cosos islands in the Indian Ocean and for Trindade, Martin Vas, Tristan da Cunha islands and Bonaparte, Gough and New England (except Atlantis) seamounts in the Atlantic Ocean. No best-fitting T_e value could be obtained for those volcanoes, either because the sub-satellite geoid signature of the seamount was too small for the observed–computed residuals to be significant (low signal to noise ratio) or because no single T_e value produced a clear minimum in the residuals, perhaps because of a wrong local bathymetry (no correlation between observed and computed geoid profiles).

ANALYSIS OF RESULTS

In Fig. 3, the t_e estimates are plotted as a function of the age of the plate at time of loading Δt. Although an increasing trend can be observed, a very large scatter is present. The scatter is mainly due to the very low estimates found in the south-central Pacific. This region has therefore been analysed separately from the rest of the oceanic domain which presents a much more coherent trend. Excluding the south-central pacific, computed a linear regression of T_e has been computed as a function of the square root of age. T_e values have been weighted according to their error bars. The following empirical relationship is obtained:

$$T_e \,(\mathrm{km}) = 2.70\sqrt{\Delta t}\,(\mathrm{Ma}). \tag{6}$$

The standard deviation of the rate, σ, is 0.15, indicating good coherency within the data set.

Many studies have been conducted in order to relate the apparent elastic thickness of the oceanic lithosphere to the temperature distribution (Murrel 1976; Goetze & Evans 1978; Lago & Cazenave 1981; Bodine, Steckler & Watts 1981; McNutt & Menard 1982; Sandwell & Schubert 1982; De Rito, Cozzarelli & Hodge 1986). Models and experiments based on mantle rock rheology (mainly olivine) agree in identification of the apparently elastic core of the oceanic lithosphere with the upper part of the lithosphere, where the temperature is less than 600 °C, implying
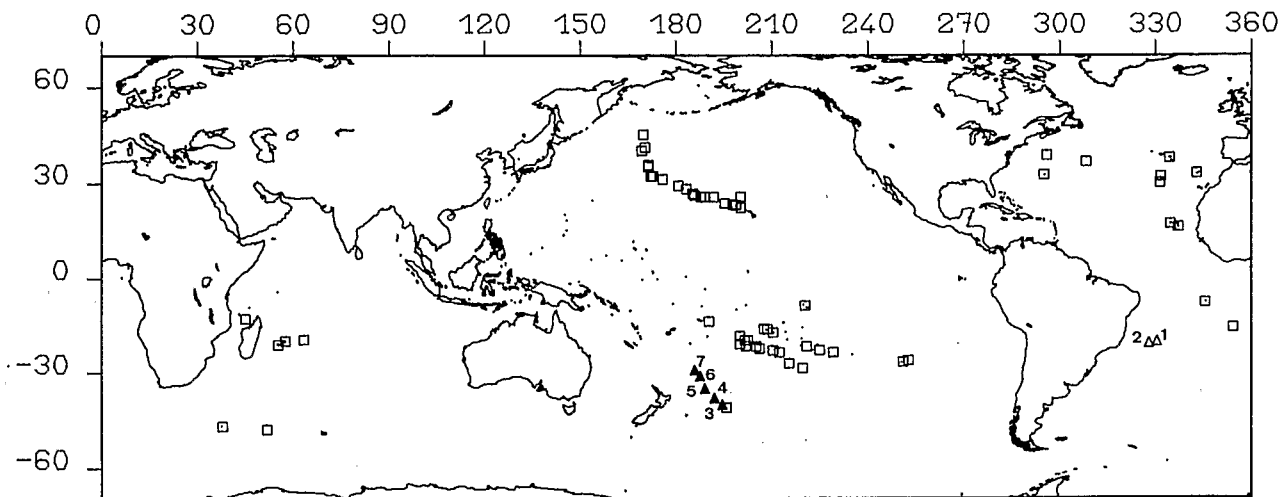
Figure 2. Location of the t_e estimates. Open squares represent volcanoes reported in Table 2. Open triangles represent volcanoes for which an age is proposed (Trindade chain). Full triangles represent location of volcanoes where a plate age is proposed (northern end of the Louisville Ridge). Numbers refer to Table 3.

thickening rates close to $4\,km\,Ma^{-1/2}$. On the other hand, the thickening rate deduced from seamounts loading is closer to $2.5–3\,km\,Ma^{-1/2}$, which correspond to an isotherm between 350 and 450 °C. The difference between the observed and predicted rates must be interpreted in terms of lithospheric geotherm since inelasticity may be ruled out (McNutt & Menard 1982; McNutt 1984). The fact that the observed rate is lower than the predicted rate indicates that an upwelling of the isotherms occurs together with volcano emplacement.

Such an upward migration of the isotherms has already been invoked to explain the bathymetric swells associated with hot-spot chains (Crough 1978). Detrick & Crough (1978) proposed to associate a thermal age (in fact a bathymetric age) to the raised lithosphere. Further, McNutt (1984) showed that when compared to this thermal age, elastic thickness estimates fit well for 550–600 °C isotherms, whereas they only fit for lower isotherms (350–450 °C) when compared to the age from isochrons. The difference between the predicted and the observed rates found in this study thus represents the mean rejuvenation of the oceanic lithosphere associated with intraplate volcanism.
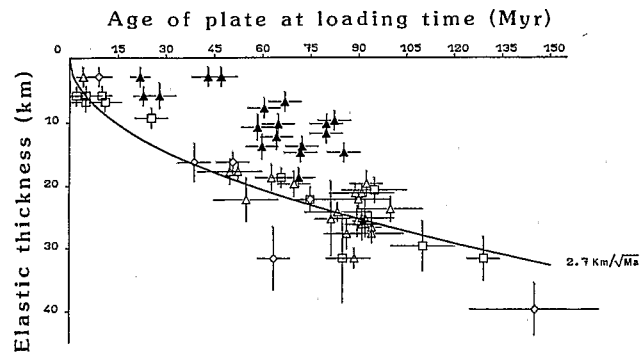
Figure 3. Elastic thickness estimates (T_e) plotted versus age of the plate at the time of loading (Δt). Squares are for the Atlantic Ocean, diamonds for the Indian Ocean and triangles for the Pacific Ocean. Full triangles are for the south-central Pacific. The solid line represents $T_e = 2.70\sqrt{\Delta t}$.

The scatter around the mean trend which is illustrated in Fig. 3 may be explained in terms of relative rejuvenation from one place to another, as previously discussed by Crough (1978) and McNutt (1984). Relative to the mean trend, excess in elastic thickness should indicate a thermal perturbation limited to the lower lithosphere. It must be noted that no estimate is close to the 600 °C isotherm (except for 0-Ma lithosphere where isotherms cannot be discriminated). This indicates that intraplate volcanism is always associated with a thermal perturbation of the lithosphere (i.e. a short-wavelength rejuvenation), even if a bathmetric swell (thermal effect on a larger scale) is not visible, or is not more visible.

This scheme does not hold in the south-central Pacific. The very low estimates found in this region argue for a major change in the thermal structure of the lithosphere. Bathymetric, seismological and gravity observations which confirm this interpretation have been reported by McNutt & Fisher (1987) and Calmant & Cazenave (1987). In contrast with the rejuvenation related to hotspot volcanism which is occurring elsewhere, lithospheric rejuvenation is on a regional scale in the south-central Pacific. In fact, the south-central Pacific may not be the only place affected by this regional rejuvenation. Smith, Watts & Pringle (1987) also found low elastic thickness estimates for Himu seamount and Hemler guyot, two volcanoes within the Darwin Rise (Menard 1984). Menard (1984) has already related the subsidence recorded in guyot depths within the Darwin Rise to the anomalous depth now observed in the south-central Pacific. Since the palaeoposition of the Darwin Rise corresponds to the actual position of the south-central Pacific, the fact that the Darwin Rise has been affected indicates that the thermal perturbation has been living for a long time [the volcanoes studied by Smith *et al.* (1987) are ~100 Ma old] and has been kept fixed in the hotspot reference (see also Smith *et al.* 1989). The thermal perturbation may also affect the Nazca plate which shows a clear depth anomaly. The slow-down of surface waves observed by Nishimura & Forsyth (1985) occurs under the Darwin Rise, the south-central Pacific and possibly the

Nazca plate. In a worldwide study of seafloor subsidence, Marty & Cazenave (1989) found that the subsidence rates for the south-central Pacific and Nazca plates are much lower than the mean value upon the whole oceanic domain (179 ± 14 and 206 ± 12 m Ma$^{-1/2}$ for the south-central Pacific and Nazca, respectively, versus 285 m Ma$^{-1/2}$ for the mean rate). The regional scale depth anomalies are then at least partly remnants of ridge processes, unrelated to the midplate hotspot volcanism.

AGE PREDICTION

Age predictions have often been used to infer the geological evolution of oceanic basins. In this way, elastic thickness determinations have been widely used. Watts *et al.* (1980) separated Pacific volcanoes into two groups; on- and off-ridge volcanoes according to small (~5 km) or large (~25 km) elastic plate thickness. Using relation (6), the tectonic setting of intraplate volcanoes may be studied more precisely. We present examples of both volcano and plate age predictions from T_e estimates of regionally compensated volcanoes. The reliability of such predictions is governed by the statistics on the regression line used. It is implicitly assumed that the amounts of thinning of the elastic layer that the lithosphere has undergone at the studied place is within the standard deviation (4 km) around the mean trend. That is not the case for the south-central Pacific plate where no reliable predictions can be obtained from relation (6).

The Trindade chain

The chain lies in the Brazil basin of the south Atlantic Ocean and may extend onto the South American continent. According to Morgan (1981), it has a hotspot origin, whose present location should be Martin Vas Island (20.5 °S, 28.9 °W). Little is known about ages along the chain except that Morgan (1981) reports an age of 60–70 Ma for lava flows on the Brazilian coast and 3 mA at Trindade Island, just west of Martin Vas Island. A T_e estimate is available for Columbia seamount, in the middle of the chain ($T_e = 20$ km, for this study, see Table 3), and a value of 20–30 km is given by Bulot *et al.* (1984) for Trindade Island. In this area, Larson *et al.* (1985) give crustal ages (Table 3) in good agreement with the kinematics of the south Atlantic derived by Sibuet & Mascle (1978) who locate magnetic anomaly 34 (82 Ma) between these two islands. Using relation (6) leads to an age of 35 ± 11 Ma for Columbia seamount and to 0–17 Ma for Trindade Island. These values agree remarkably well with the hotspot backtrackings of Morgan (1981) and Duncan (1981) who both infer an age between 20 and 40 Ma for Columbia seamount. The age of Trindade Island (3 Ma) is within the wide range computer from the T_e estimate of Bulot *et al.* (1984).

The Pacific plate along the northern part of the Louisville Ridge

Recent studies have focused on the Louisville Ridge. Volcano ages are reported by Lonsdale (1988) and have been interpolated along the chain. T_e estimates have been carried out by Cazenave & Dominh (1984) and by Watts *et al.* (1988). The tectonic setting of the chain is quite well constrained for the southern part of the chain up to Valerie Guyot (Watts *et al.* 1988) but is unclear further to the northwest since no magnetic anomalies have been reported for this part of the Pacific plate. Plate age estimates have been made by Menard *et al.* (1983) and by the leg 91 scientific party (1983) for the area of deep-sea drilling sites 595–596 near 23.8 °S–165.5 °W. A spreading direction has also been inferred from seismic anisotropy experiments (Shearer & Orcutt 1985). Both the age (130–150 Ma) and the former ridge direction (030°) imply that the ocean floor in the region of leg 91 was created by a ridge other than the Pacific–Antarctic Ridge.

In addition to Valerie Guyot (included in the worldwide study), Cazenave & Dominh (1984) provided estimates of T_e for five volcanoes located further west. Two sets of estimates are proposed, depending on whether a 2-D (admittance) or a 3-D (as in this paper) model is used. The data used were along-track SEASAT geoid heights and the bathymetric map of Mammerickx *et al.* (1974). Recently, Watts *et al.* (1988) published new T_e estimates. These estimates are mainly based on gravimetric and bathymetric shipboard data using a 2-D (admittance) model. All of these estimates are displayed in Table 3. A noticeable scatter is present, mostly for the southernmost volcanoes. Two reasons may be invoked to explain the differences; systematic bias due to the different models and the data.

Ribe (1982) has provided an extended study of the bias which may occur when the admittance technique is used to determine a value of T_e. He has shown that the aspect ratio of the load, χ, ($\chi = 1$ when the volcanic edifice is circular and $\chi \to \infty$ when it is part of a continuous ridge) is a key factor. Computations of the admittance function from bathymetric and gravimetric (or geoid height) profiles over the summit of a volcano assume that the load is infinitely long in a direction normal to the profiles ($\chi \to \infty$). Thus, for a given plate deflection, this over-estimation of the load

Table 3. Plate or volcano ages (t_p and t_v respectively) assumed using relation (6) for the listed volcanoes and the associated elastic thicknesses T_e. * denotes the inferred value.

Location		Age of plate (Ma)	Age of volcano (Ma)	Elastic thickness T_e (km)
Trindade chain				
1. Columbia	21.0°S 32.0°W	20±2[5]	90	35±4*
2. Trindade	20.5°S 29.5°W	20–30[1]	75	0–17*
Louisville Ridge				
3. Currituck	30.0°S 173.5°W	22.4±.75[2] 12.5–17.5[4]	131±22*	62±2
4. Lousiville	31.4°S 172.3°W	20.4±1.4[2] 15–20[3] 10–20[4]	115±24*	58±2
5. Forde	35.4°S 170.8°W	15.8±3[2] 15[4]	83±40*	49±1
6. LR2	38.4°S 167.8°W	17.8±1.2[2] 12–15[3] 34–41[4]	85±20*	42
7. LR1	40.6°S 165.3°W	17.2±.65[2] 37.5–32.5[4]	76±14*	35.5

1: Bulot et al., 1984
2: Cazenave and Dominh, 1984 (3D estimates)
3: Cazenave and Dominh, 1984 (2D estimates)
4: Watts et al., 1988
5: This study

results in an over-estimation of the plate stiffness. To first order, the fact that the agreement between the different estimates is better in the north than in the south may be interpreted in terms of a difference of aspect ratio of the volcanoes along the chain; this is very large for the ridge segments in the north, whereas it is closer to 1 for the isolated peaks in the south. Watts *et al.* (1988) show (fig. 19 in their paper) how the estimate of the best fitting value of T_e varies with the aspect ratio assumed for LR1 seamount. This best fitting value increases from ~11 km at $\chi = 1$ to ~40 km when $\chi \rightarrow \infty$. Taking the 2000-fathom isobath as the foot of the seamount (Watts *et al.* 1988, fig. 4), LR1 seems to have in fact an aspect ratio of 3:1. A rough extrapolation leads to a T_e value around 15–20 km for such a value of χ, in agreement with the 17.2 ± 0.7 km proposed by Cazenave & Dominh (1984). Hence, for the southernmost isolated peaks, the aspect ratio seems to account for most of the difference between the 2-D and 3-D estimates. In the north, good agreement is found for Louisville seamount. No explanation of why the 2-D estimate by Watts *et al.* (1988) for Currituck is slightly lower than the 3-D estimate from Cazenave & Dominh (1984) has been found. Errors in the data are not likely since a fine coverage of the seamount is already reported in the map of Mammerickx *et al.* (1974), used by Cazenave & Dominh (1984). The densities are the same in both studies. Cazenave & Dominh (1984) failed to determine a 2-D estimate of T_e for this volcano because the signal-to-noise ratio was too low, although the estimates seem particularly well constrained in the 3-D computation (Cazenave & Dominh 1984). In fact, Currituck is a rather small volcano, with little energy in the 50–150 km waveband—the most discriminant waveband in compensation analyses—and consequently is badly constrained in spectral analyses. Last, when using the admittance technique, it is assumed that the sampled depth is representative of the maximum height reached by the volcano. If this is not the case, i.e. if the profile passed through a saddle within the northern ridge, the admittance function is computed with an under-estimated depth (relative to the sampled gravimetry), leading to an under-estimation of T_e (Ribe 1982). The location of the ship tracks, displayed by Watts *et al.* (1988) in their fig. 4 is not precise enough to test this hypothesis. Hence, according to the previous discussion, we have preferred to use the 3-D estimates of T_e to infer ages from relation (6). In the following section, we use these estimates to determine the the Pacific plate along the chain since the age of the volcanoes is better constrained.

From LR1 to Forde seamounts, the inferred plate ages are within the range 75–85 Ma. This is in a relatively good agreement with the extrapolation proposed by Watts *et al.* (1988) who suggest that the plate ages along the chain should only slightly increase ($t_p \sim 80$ Ma) northwest of Valerie Guyot (Fig. 4). Values for the plate underlying Louisville and Currituck seamounts, $t_p = 115 \pm 24$ and 131 ± 22 Ma respectively, are much higher and present a clear age offset with plate ages up to Forde seamount. This can be explained if a different ridge had generated the underlying crust. Menard *et al.* (1983) proposed that the area of leg 91 represents an abandoned fragment of the Antarctic plate. Mammerickx (1986) suggests that the region north of the Louisville Ridge and west of a topographic
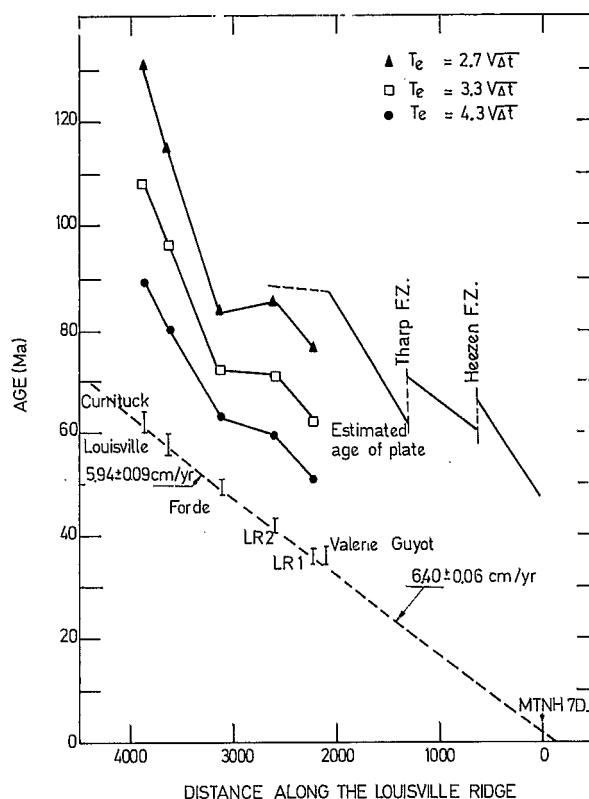
Figure 4. Ages for volcanoes along the Louisville Ridge with the age pattern along the ridge (dashed line), plate ages using magnetic isochrons southeast of Valerie Guyot and the inferred plate ages northwest of Valerie Guyot using the 2.70 (this study), 3.3 and 4.3 (olivine rheology) rates of elastic layer thickening with age of the lithosphere. MTHN-70 volcano is the youngest dated volcano, close to the hotspot location as proposed by Lonsdale (1988). Redrawn from Watts *et al.* (1988).

lineament connecting the eastern edge of Campbell plateau to the eastern edge of Manihiki plateau along 165 °W represents a large segment of abandoned Phoenix plate. Although the former plate setting is not clear, our study suggests that the eastern boundary of this old Pacific crust runs within 32–34 °S, 171–172 °W.

The thickening rates derived by Bodine *et al.* (1981) from the rheology of olivine (3.3 and 4.3 km Ma$^{-1/2}$ respectively for wet and dry olivine) lead to unrealistic plate ages between LR1 and Forde seamounts (see Fig. 4). Along the Trindade chain, these rates would have led to an age of 53–68 Ma for Columbia seamount using wet and dry olivine rheology respectively. These values may be rejected since they imply a very irregular age progression along the chain, incompatible with the other hotspot tracks in the south Atlantic. Both examples give justification to using the relationship proposed in this paper which takes into account—although empirically and to first order—the thermal effect of the seamount emplacement on the lithospheric mechanical response.

CONCLUSION

According to its apparent elastic thickness, the oceanic lithosphere may be separated into two areas: the first one is

centred on the south-central Pacific and may include the Darwin Rise area and the Nazca plate and the second comprises the rest of the oceans. Within the first area, elastic thickness is generally very small and presents no particular trend with age. The other estimates show a clear increase with age that was adjusted with a square root of age relationship. The low value ($2.7 \, \text{km} \, \text{Ma}^{-1/2}$) found for the rate indicates that a noticeable rejuvenation of the lithosphere accompanies mid-plate volcanism. The deviations around the mean trend may be attributed in part to the thermal effects of the volcano emplacement, which may be variable. The standard deviation (0.15) of the computed rate makes it possible to predict either volcano or plate ages with reliability using the proposed relationship. The good fit which has been demonstrated in two examples has to be considered in the light of the large uncertainties which bracket the predicted values. The predictions should be checked with respect to the geodynamical framework, but should not be used to inder that geodynamical setting.

Two limitations must be stressed; the use of the trend is unsuitable in the anomalous areas outlined above and biased ages will result from 2-D estimates of T_e unless aspect ratio of the load is taken into account.

ACKNOWLEDGMENTS

REFERENCES

Bodine, J. H., Steckler, M. S. & Watts, A. B., 1981. Observations of flexure and the rheology of the oceanic lithosphere, *J. geophys. Res.*, **86**, 3695–3707.

Bulot, A., Diament, M., Kogan, M. G. & Dubois, J., 1984. Isostasy of aseismic tectonic units in the South Atlantic Ocean and geodynamic implications, *Earth planet. Sci. Lett.*, **70**, 346–354.

Calmant, S., 1987. The elastic thickness of the lithosphere in the Pacific Ocean, *Earth planet. Sci. Lett.*, **85**, 277–288.

Calmant, S. & Cazenave, A., 1986. The effective elastic lithosphere under the Cook–Austral and Society islands, *Earth planet. Sci. Lett.*, **77**, 187–202.

Calmant, S. & Cazenave, A., 1987. Anomalous elastic thickness of the oceanic lithosphere in the south Central Pacific, *Nature*, **328**, 236–238.

Cazenave, A. & Dominh, K., 1984. Geoid height over the Louisville Ridge, *J. geophys. Res.*, **89**, 11 171–11 179.

Cazenave, A., Lago, B., Dominh, K. & Lambeck, K., 1980. On the response of the oceanic lithosphere to seamounts loads from Geos-3 satellite radar altimeter observations, *Geophys. J. R. astr. Soc.*, **63**, 233–252.

Crough, S. T., 1978. Thermal origin of mid-plate hotspot swells, *Geophys. J. R. astr. Soc.*, **55**, 1975–1988.

De Rito, R., Cozzarelli, F. A. & Hodge, D. S., 1986. A forward approach to the problem of non-linear viscoelasticity and the thickness of the mechanical lithosphere, *J. geophys. Res.*, **91**, 8295–8313.

Detrick, R. S. & Crough, S. T., 1978. Island subsidence, hotspots and lithospheric thinning, *J. geophys. Res.*, **83**, 1236–1244.

Duncan, R. A., 1981. Hotspots in the Southern Oceans—An absolute frame of reference for motion of Gondwana continents, *Tectonophysics*, **74**, 29–42.

Duncan, R. A. 1984. Age progressive volcanism in the New

England seamounts and the opening of the Central Atlantic Ocean, *J. geophys. Res.*, **89**, 9980–9990.

Emerick, C. M. & Duncan, R. A., 1982. Age progressive volcanism in the Comores archipelago, Western Indian Ocean, and implications for Somali plate tectonics, *Earth planet. Sci. Lett.*, **60**, 415–428.

Goetze, C. & Evans, B., 1978. Stress and temperature in the bending lithosphere as constrained by experimental rock mechanisms, *Geophys. J. R. astr. Soc.*, **59**, 463–478.

Harris, C., Bell, J. D. & Atkins, F. B., 1983. Isotopic composition of lead and strontium in lavas and coarse grained blocks from Ascencion Island, South Atlantic—An Addendum, *Earth planet Sci. Lett.*, **63**, 139–141.

Lago, B. and Cazenave, A., 1981. State of stress in the oceanic lithosphere in response to loading, *Geophys. J. R. astr. Soc.*, **64**, 785–799.

Larson, R. L., Pitman, W. C., Golovchenko, X., Cande, S. C., Dewey, J. F., Haxby, W. F. & Labrecque, J. L., 1985. *The Bedrock Geology of the World*, W. H. Freeman & company, New York.

Leg 91 Scientific Party, 1983. Leg 91 Tonga trench, Joides, J., **9**, 22–38.

Lonsdale, P., 1988. Geography and history of the Louisville hotspot chain in the Southwest Pacific, *J. geophys. Res.*, **93**, 3078–3104.

Mammerickx, J., 1986. Old Pacific crust in the Southwest Pacific, in *Report of the Workshop on Future Scientific Pacific Drilling in the South Pacific and Antarctic Margin*, 145, April 20–22, Gainesville, Florida.

Mammerickx, J., Smith, S. M., Taylor, I. L. & Chase, T. C., 1974. *Bathymetry of the South Pacific, report, La Jolla Institute for Marine Resources*, University of California, San Diego.

Marty, J. C. & Cazenave, A., 1989. Regional variations in subsidence rate of oceanic plates: A global analysis, *Earth Pl. Sci. Lett.*, **94**, 301–315.

McDougall, I. & Chamalaun, F. G., 1969. Isotopic dating and geomagnetic polarity studies on volcanic rocks from Mauritius, Indian Ocean, *Geol. Soc. Am. Bull.*, **80**, 1419–1442.

McNutt, M., 1984. Lithospheric flexure and thermal anomalies, *J. geophys. Res.*, **89**, 11180–11194.

McNutt, M. & Menard, H. W., 1982. Constraints on yield strength in the oceanic lithosphere derived from observations of flexure, *Geophys. J. R. astr. Soc.*, **71**, 363–394.

McNutt, M. & Fisher, K., 1987. The South Central Pacific superswell, in *Seamounts; Islands and Atolls*, Geophysical Monograph # 43, eds Keating, B. H., Fryer, P., Batiza, R. & Boehlert, G. W., Am. Geophys. Un., Washington DC.

Menard, H. W., 1984. Darwin Reprise, *J. geophys. Res.*, **89**, 9960–9968.

Menard, H. W. & McNutt, M., 1982. Evidence for and consequences of thermal rejuvenation, *J. geophys. Res.*, **87**, 8570–8580.

Menard, H. W., Jordan, T. H., Natland, J. H. & Orcutt, J. A., 1983. Tectonic evolution of the southwestern tropical Pacific basin, leg 91 scientific party, *EOS*, **84** (18), 315.

Morgan, W. J., 1981. Hotspot tracks and the opening of the Atlantic and Indian Oceans, in the Sea **7**, 443–487, ed. Emiliani, C., J. Wiley & Sons, New York.

Murrel, S. A. F., 1976. Rheology of the lithosphere, experimental indications, *Tectonophysics*, **36**, 5–24.

Nishimura, C. E. & Forsyth, D. W., 1985. Anomalous Love waves phase velocities in the Pacific: Sequential pure-path and spherical harmonics inversion, *J. geophys. Res.*, **81**, 389–407.

Reigber, C., Balmino, G., Muller, H., Bosch, W. & Moynot, B., 1985. GRIM gravity model improvement using Lageos (GRIM3-L1), *J. geophys. Res.*, **90**, 9285–9299.

Ribe, N. M., 1982. On the interpretation of frequence response functions for oceanic gravity and bathymetry, *Geophys. J. R. astr. Soc.*, **70**, 273–294.

Sandwell, D. & Schubert, G., 1982. Lithospheric flexure at fracture zones, *J. geophys. Res.*, **87**, 4657–4667.

Shearer, P. & Orcutt, J. A., 1985. Anisotropy of the oceanic lithosphere. Theory and observations from the Ngendei seismic refraction in the Southwest Pacific, *Geophys. J. R. astr. Soc.*, **80**, 493–526.

Sibuet, J. C. & Mascle, J., 1978. Plate kinematic implications of Atlantic Equatorial fracture zone trends, *J. geophys. Res.*, **83**, 3401–3421.

Smith, W. H., Watts, A. B. & Pringle, M., 1987. Evidence from Cretaceous seamounts for the longevity of geophysical and geochemical anomalies of French Polynesia, *EOS Trans. Am. Geophys. Un.*, **68**, 1446.

Smith, H. W., Staudigel, H., Watts, A. B. & Pringle, M. S., 1989. The Magellan Seamounts: Early Cretaceous record of the South Pacific isotopic and thermal anomaly, *J. geophys. Res.*, **94**, 10 501–10 523.

Van Wickhouse, R. J., 1973. *SYNBAPS (SYNthetic BAthymetric Profiling Systems)*, Technical Report of the Naval Oceanographic Office, Washington, D.C.

Walcott, R. I., 1970. Flexure of the lithosphere at Hawaii, *Tectonophysics*, **9**, 435–446.

Watts, A. B., 1978. An analysis of isotasy in the world's oceans: 1. Hawaii-Emperor seamount chain, *J. geophys. Res.*, **83**, 5989–6004.

Watts, A. B., 1979. On geoid heights derived from geos-3 altimeter data and flexure of the lithosphere along the Hawaiian-Emperor seamount chain, *Geophys. J. R. astr. Soc.*, **38**, 119–141.

Watts, A. B. & Cochran, J. R., 1974. Gravity anomalies and flexure of the lithosphere along the Hawaii-Emperor seamount chain, *Geophys. J. R. astr. Soc.*, **38**, 119–141.

Watts, A. B. & Ribe, N. M., 1984. On geoid height and flexure at seamounts, *J. geophys. Res.*, **89**, 11152–11170.

Watts, A. B., Cochran, J. R. & Selzer, G., 1975. Gravity anomalies and flexure of the lithosphere: A three dimensional study of the Great Meteor seamount, *Northeast Atlantic, J. geophys. Res.*, **80**, 1391–1398.

Watts, A. B., Bodine, J. H. & Ribe, N. M., 1980. Observation of flexure and the geophysical evolution of the Pacific ocean basin, *Nature*, **283**, 532–537.

Watts, A. B., Weissel, J. K., Duncan, R. A. & Larson, R. L., 1988. The origin of the Louisville ridge and its relationship to the Eltanin Fracture Zone system, *J. geophys. Res.*, **93**, 3051–3077.

Young, R. & Hill, I. A., 1986. An estimate of the effective elastic thickness of the Cape Verde Rise, *J. geophys. Res.*, **91**, 4854–4866.